

Calculation of the nucleon sigma term and strange quark content with two flavors of dynamical overlap fermions

**H. Ohki^{*a,b}, H. Fukaya^c, S. Hashimoto^{d,e}, H. Matsufuru^d, J. Noaki^d, T. Onogi^b,
E. Shintani^d, N. Yamada^{d,e} (for JLQCD collaboration)**

^aDepartment of Physics, Kyoto University, Kyoto 606-8501, Japan,

^bYukawa Institute for Theoretical Physics, Kyoto University, Kyoto 606-8502, Japan,

^cThe Niels Bohr Institute, The Niels Bohr International Academy Blegdamsvej 17 DK-2100
Copenhagen, Denmark,

^dHigh Energy Accelerator Research Organization (KEK), Tsukuba 305-0801, Japan,

^eSchool of High Energy Accelerator Science, The Graduate University for Advanced Studies
(Sokendai), Tsukuba 305-0801, Japan,

E-mail: ohki@yukawa.kyoto-u.ac.jp

We present a calculation of the nucleon sigma term on two-flavor QCD configurations with dynamical overlap fermions. We analyse the lattice data for the nucleon mass using the baryon chiral perturbation theory. Using partially quenched data sets, we extract the connected and disconnected contributions to the nucleon sigma term separately. Chiral symmetry on the lattice simplifies the determination of the disconnected contribution. We find that the strange quark content, which determines the neutralino dark matter reaction rate with nucleon through the Higgs boson exchange, is much smaller than the previous lattice results.

The XXVI International Symposium on Lattice Field Theory

July 14-19 2008

Williamsburg, Virginia, USA

*Speaker.

1. Introduction

Nucleon sigma term $\sigma_{\pi N}$ is given by a scalar form factor of nucleon at zero recoil. While up and down quarks contribute to $\sigma_{\pi N}$ both as valence and sea quarks, strange quark appears only as a sea quark contribution. As a measure of the strange quark content of the nucleon, the y parameter is commonly introduced. These parameters are defined as

$$\sigma_{\pi N} = m_{ud} \langle N | \bar{u}u + \bar{d}d | N \rangle, \quad y \equiv \frac{2 \langle N | \bar{s}s | N \rangle}{\langle N | \bar{u}u + \bar{d}d | N \rangle}. \quad (1.1)$$

The y parameter plays an important role to determine the detection rate of possible neutralino dark matter in the supersymmetric extension of the Standard Model [1, 2, 3, 4, 5]. Already with the present direct dark matter search experiments one may probe a part of the MSSM model parameter space, and new experiments such as XMASS and SuperCDMS will be able to improve the sensitivity by 2–3 orders of magnitude. Therefore, a precise calculation of the y parameter will be important for excluding or proving the neutralino dark matter scenario.

Using lattice QCD, one can calculate the nucleon sigma term directly. Furthermore, it is possible to determine the valence and sea quark contributions separately. Previous lattice results were $\sigma_{\pi N} = 40\text{--}60$ MeV, $y = 0.66(15)$ [6], and $\sigma_{\pi N} = 50(3)$ MeV, $y = 0.36(3)$ [7] within the quenched approximation, while a two-flavor QCD calculation [8] gave $\sigma_{\pi N} = 18(5)$ MeV and $y = 0.59(13)$. There is an apparent puzzle in these results: the strange quark content is unnaturally large compared to the up and down contributions that contain the connected diagrams too.

Concerning this problem, it was pointed out that using the Wilson-type fermions, the sea quark mass dependence of the additive mass renormalization and lattice spacing can give rise to a significant lattice artifacts in the sea quark content [9]. Unfortunately, after subtracting this contamination the unquenched result has large statistical error, $y = -0.28(33)$.

In this study, we analyze the data of the nucleon mass obtained from a two-flavor QCD simulation employing the overlap fermion [10] which can remove this problem by explicitly maintaining exact chiral symmetry on the lattice. Although the two-flavor QCD calculation cannot avoid the systematic error due to the neglected strange sea quarks, our study with exact chiral symmetry reveals the underlying systematic effects in the calculation of the nucleon sigma term, especially in the extraction of its sea quark contribution. It therefore provides a realistic test case, which will be followed by 2+1-flavor calculations in the near future ¹. The full details of this work is presented in [11].

2. Lattice simulation

We make an analysis of the nucleon mass obtained by two-flavor QCD configurations generated with dynamical overlap fermions. Our simulations are performed at a lattice spacing $a = 0.118(2)$ fm on a $16^3 \times 32$ lattice with a trivial topological sector $Q = 0$. For each sea quark mass, we accumulate 10,000 trajectories; the calculation of the nucleon mass is done at every 20 trajectories, thus we have 500 samples for each m_{sea} . For the sea quark mass am_{sea} we take six values:

¹For a very recent result from 2+1-flavor QCD, see [12].

0.015, 0.025, 0.035, 0.050, 0.070, and 0.100 that cover the mass range $m_s/6 - m_s$ with m_s the physical strange quark mass. Analysis of the pion mass and decay constant on this data set is found in [13]. In order to improve the statistical accuracy, we use the low-mode preconditioning technique. The two-point function made of low-lying modes of the overlap-Dirac operator is averaged over different time slices with 50 chiral pairs of the low modes. For the quark propagator, we take a smeared source defined by a function $\phi(|\vec{x}|) \propto \exp(-A|\vec{x}|)$ with a fixed $A = 0.40$. We then calculate the smeared-local two-point correlator and fit the data with a single exponential function after averaging over forward and backward propagating states in time. we take the valence quark masses $am_{\text{val}} = 0.015, 0.025, 0.035, 0.050, 0.060, 0.070, 0.080, 0.090, \text{ and } 0.100$.

The matrix element defining the nucleon sigma term can be related to the quark mass dependence of the nucleon mass using the Feynman-Hellman theorem, which derives the relations between the nucleon mass and the quark contents of the nucleon as

$$\frac{\partial M_N}{\partial m_{\text{val}}} = \langle N | (\bar{u}u + \bar{d}d) | N \rangle_{\text{conn}}, \quad \frac{\partial M_N}{\partial m_{\text{sea}}} = \langle N | (\bar{u}u + \bar{d}d) | N \rangle_{\text{disc}}. \quad (2.1)$$

The subscripts ‘‘conn’’ and ‘‘disc’’ on the expectation values indicate that only the connected or disconnected quark line contractions are evaluated, respectively. In the present study we exploit this indirect method to extract the matrix elements corresponding to the nucleon sigma term.

Another possible method is to directly calculate the matrix element from three-point functions with an insertion of the scalar density operator $(\bar{u}u + \bar{d}d)(x)$. In principle, it gives a mathematically equivalent result to the indirect method including lattice artifacts. Numerical differences could arise only in the statistical error and the systematic uncertainties of the fit ansatz.

3. Analysis of the unitary points with baryon chiral perturbation theory

We carry out baryon chiral perturbation theory (BChPT) [14] fits of the nucleon mass at the five heaviest quark masses for unitary point by using a simplified fit function

$$M_N = M_0 - 4c_1 m_\pi^2 - \frac{3g_A^2}{32\pi f_\pi^2} m_\pi^3 + e_1^r(\mu) m_\pi^4, \quad (3.1)$$

where M_0 is the nucleon mass in the chiral limit and f_π is the pion decay constant fixed at its physical value 92.4 MeV and the constant g_A describes the nucleon axial-vector coupling. Since the coupling g_A is very well known experimentally, we attempt two options: (Fit a) a fit with fixed $g_A (=1.267)$, and (Fit b) a fit with g_A being dealt as a free parameter. Moreover we also carry out the full $\mathcal{O}(p^3)$ fit and $\mathcal{O}(p^4)$ fit following the analysis done in [15]. The left panel of Fig. 1 shows the BChPT fits. The lattice data show a significant curvature towards the chiral limit. All the details of our analysis can be found in [11].

In order to estimate the systematic uncertainties due to the finite volume effect, we correct the data for the finite volume effect using BChPT $\mathcal{O}(p^4)$ formula [16]. For the input parameters M_0 , g_A , c_1 , we use the nominal values ($M_0 = 0.87$ GeV, $g_A = 1.267$, $c_1 = -1.0$ GeV $^{-1}$). The chiral fit is then made for the corrected data points using the formula (3.1) for the five or six heaviest data points. The result is shown in the right panel of Fig. 1. After correcting the finite volume effect, there are 5-8% decrease in M_0 and 4-7% increase in the magnitude of the slope $|c_1|$. We observe that the deviation due to the finite volume effect is smaller than the uncertainty of the fit forms.

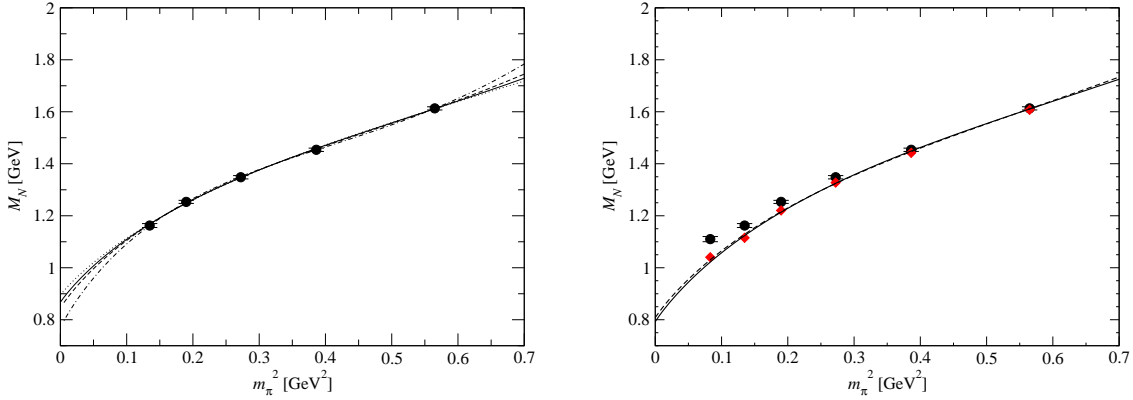


Figure 1: Chiral fit of the lattice raw data (left) and the corrected data (right). In the left panel, the solid curve represents the Fit a. The dot, dashed, dot-dashed curves correspond to the fits using BChPT including higher order terms. In the right panel, Solid and dashed curves represent the fits using 5 and 6 heaviest data points (diamond), respectively. For a reference, we also show the raw data (circles).

Taking the Fit a (g_A fixed, Finite volume corrections not included) as our best fit and using the variation with fit ansatz and Finite volume corrections as an estimate of the systematic errors, our result of the nucleon sigma term is

$$\sigma_{\pi N} = 52(2)_{\text{stat}} \left(\begin{smallmatrix} +20 \\ -7 \end{smallmatrix} \right)_{\text{extrap}} \left(\begin{smallmatrix} +5 \\ -0 \end{smallmatrix} \right)_{\text{FVE}} \text{ MeV}, \quad (3.2)$$

where the errors are the statistical and the systematic due to the chiral extrapolation (extrap) and finite volume effect (FVE). The largest uncertainty comes from the chiral extrapolation. The finite volume effect is sub-leading, which is about 9%. This result is in good agreement with the phenomenological analysis based on the experimental data.

4. Partially quenched analysis and extraction of y

In order to extract the connected and disconnected diagram contributions separately, we fit the quark mass dependence of the nucleon mass with the one-loop partially quenched ChPT formula [17]

$$\begin{aligned} M_N = & B_{00} + B_{10}(m_{\pi}^{vv})^2 + B_{01}(m_{\pi}^{ss})^2 + B_{20}(m_{\pi}^{vv})^4 + B_{11}(m_{\pi}^{vv})^2(m_{\pi}^{ss})^2 + B_{02}(m_{\pi}^{ss})^4 \\ & - \frac{1}{16\pi f_{\pi}^2} \left\{ \frac{g_A^2}{12} [-7(m_{\pi}^{vv})^3 + 16(m_{\pi}^{vs})^3 + 9m_{\pi}^{vv}(m_{\pi}^{ss})^2] + \frac{g_1^2}{12} [-19(m_{\pi}^{vv})^3 + 10(m_{\pi}^{vs})^3 + 9m_{\pi}^{vv}(m_{\pi}^{ss})^2] \right. \\ & \left. + \frac{g_1 g_A}{3} [-13(m_{\pi}^{vv})^3 + 4(m_{\pi}^{vs})^3 + 9m_{\pi}^{vv}(m_{\pi}^{ss})^2] \right\} \end{aligned} \quad (4.1)$$

where m_{π}^{vv} , m_{π}^{vs} , and m_{π}^{ss} denote the pion mass made of valence-valence, valence-sea, and sea-sea quark combinations, respectively. At this order, one can rewrite the expression in terms of m_{val} and m_{sea} using the leading-order relations. The coupling constant g_1 is another axial-vector coupling. We use nominal values $g_A = 1.267$ and $g_1 = -0.66$ when they are fixed in the fit. There are also contributions from the decuplet baryons. In our analysis these contributions can be absorbed into the analytic terms in (4.1). The independent fit parameters are B_{00} , B_{01} , B_{10} , B_{11} , B_{20} , B_{02} , g_1 , and g_A . We attempt a fit with fixed g_A and g_1 (Fit PQ-a), a fit with fixed g_A (Fit PQ-b) and a fit with all the free parameters (Fit PQ-c). Finite volume corrections are not taken into account.

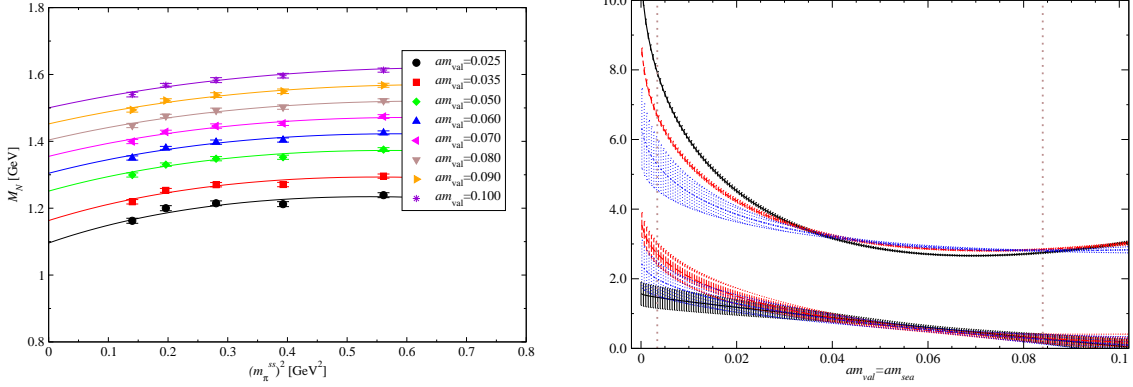


Figure 2: The left panel shows partially quenched nucleon masses and fit curves (Fit PQ-b). The right panel shows the connected (up) and disconnected (down) contributions to the sigma term evaluated at $m_{val} = m_{sea}$. Solid, dashed and dotted curves represent the results from the Fit PQ-a, PQ-b and PQ-c, respectively. The two vertical lines show physical up and down quark mass $am_q = 0.0034$ (left) and strange quark mass $am_q = 0.084$ (right).

The left panel of Fig. 2 demonstrates the result of the partially quenched ChPT fit. The sea quark mass dependence at eight fixed valence quark masses are nicely fitted with the formula (4.1). We find that both axial-couplings can be determined with reasonable accuracy ($g_A = 0.93(22)$ and $g_1 = -0.29(5)$) for the Fit PQ-c. The right panel of Fig. 2 shows the partial derivatives in (2.1) with respect to m_{val} and to m_{sea} evaluated at the unitary points $m_{val} = m_{sea}$. For both contributions, we clearly find an enhancement towards the chiral limit. Results with different fit ansatz show slight disagreement near the chiral limit, which indicate the size of the systematic uncertainty. We find that the sea quark content of the nucleon $\langle N | (\bar{u}u + \bar{d}d) | N \rangle_{disc} / \langle N | (\bar{u}u + \bar{d}d) | N \rangle_{conn}$ is less than 0.4 for the entire quark mass region in our study, so that the valence quark content is the dominant contribution to the sigma term.

Rigorously speaking, it is not possible to extract the strange quark content $\langle N | \bar{s}s | N \rangle$ within two-flavor QCD. Instead, in this work, we provide a ‘‘semi-quenched’’ estimate of the strange quark content which is defined as the ratio of the strange quark content (disconnected contribution at $m_{val} = m_{sea} = m_s$) to the up and down quark contributions (connected plus disconnected contributions at $m_{val} = m_{sea} = m_{ud}$) following [9]. Taking the result from the Fit PQ-b as a best estimate, we obtain the parameter y as

$$y^{N_f=2} = 0.030(16)_{stat} \begin{pmatrix} +6 \\ -8 \end{pmatrix}_{extrap} \begin{pmatrix} +1 \\ -2 \end{pmatrix}_{m_s}, \quad (4.2)$$

where the errors are statistical and systematic from chiral extrapolation and from the uncertainty of m_s , respectively. The chiral extrapolation error is estimated by the differences of the results of Fit PQ-a,b and c. We also note that there may be an additional $\sim 10\%$ error from the finite volume effect as discussed in Section 3, but it is much smaller than the statistical error in our calculation.

5. Discussion and summary

We found that the disconnected contribution to the sigma term is much smaller than the previous lattice calculations with the Wilson-type fermions $y \simeq 0.36 \sim 0.66$ [6, 7, 8] (except for [9] as



Figure 3: Two-loop diagrams for the mass shift and the operator mixing involving both the valence and the sea quarks. These graphs show the corresponding contribution to the sigma term. Due to the power divergent mass shift, the flavor singlet sea quark scalar operator insertion contributes as the flavor singlet scalar operator insertion with coefficient of additive mass shift.

explained below). The authors of [9] found that the naive calculation with the Wilson-type fermions may over-estimate the sea quark content due to the mixing effect from the additive mass shift as

$$\left. \frac{\partial M_N}{\partial m_{\text{sea}}^{\text{bare}}} \right|_{m_{\text{val}}^{\text{bare}}} = Z_m \left[\left. \frac{\partial M_N}{\partial m_{\text{sea}}^{\text{phys}}} \right|_{m_{\text{val}}^{\text{phys}}} + \left. \frac{\partial m_{\text{val}}^{\text{phys}}}{\partial m_{\text{sea}}^{\text{bare}}} \right|_{m_{\text{val}}^{\text{bare}}} \cdot \left. \frac{\partial M_N}{\partial m_{\text{val}}^{\text{phys}}} \right|_{m_{\text{sea}}^{\text{phys}}} \right], \quad (5.1)$$

where Z_m is the renormalization factor of the quark mass. Therefore, in order to obtain the derivative (2.1) one must subtract the unphysical contribution from the additive mass. They found that their unsubtracted result $y = 0.53(12)$ is substantially reduced and becomes consistent with zero: $y = -0.28(33)$. It should be noted that this mixing effect is not limited to the spectrum method but arises also in the direct matrix element method. It is easy to see that the operator is indeed a derivative of the mass shift with respect to the sea quark mass so that

$$(\bar{\psi}\psi)_{\text{sea}}^{\text{bare}} = Z_m \left[(\bar{\psi}\psi)_{\text{sea}}^{\text{phys}} + \left. \frac{\partial m_{\text{val}}^{\text{phys}}}{\partial m_{\text{sea}}^{\text{bare}}} \right|_{m_{\text{val}}^{\text{bare}}} (\bar{\psi}\psi)_{\text{val}}^{\text{phys}} \right] \quad (5.2)$$

holds. (Subtraction of the divergent counter terms is assumed on the left hand side.) Fig. 3 shows the two-loop contribution of the operator mixing of the bare sea quark operator with physical valence quark operator due to the additive mass shift which arises from the absence of the chiral symmetry. Our calculation using the overlap fermion is free from this artifact because of the exact chiral symmetry. Therefore, the small value of y obtained in our analysis (4.2) provides a much more reliable estimate than the previous lattice calculations ².

In summary, we have calculated the nucleon sigma term and the strange quark content of nucleon in two-flavor QCD simulation on the lattice with exact chiral symmetry. Owing to the exact chiral symmetry, our lattice calculation is free from the large lattice artifacts coming from the additive mass shift present in the Wilson-type fermion formulations. From an analysis of partially quenched lattice data, we have found that the sea quark content of the nucleon is less than 0.4 for the entire quark mass region in our study.

An obvious extension of this work is the calculation including the strange quark loop in the vacuum. Simulations with two light and one strange dynamical overlap quarks are on-going [19].

²Strictly speaking, there is another artifact from the sea quark mass dependence of the lattice spacing. We have found that the lattice spacing dependence is negligibly small, since we exploit mass-independent renormalization scheme (c.f. [18]) in contrast to [9], in which they used the Sommer scale for the scale input at each sea quark mass.

The main numerical calculations were performed on IBM System Blue Gene Solution at High Energy Accelerator Organization (KEK) under support of its Large Scale Simulation Program (No. 07-16). We also used NEC SX-8 at Yukawa Institute for Theoretical Physics (YITP), Kyoto University and at Research Center for Nuclear Physics (RCNP), Osaka University. The simulation also owes to a gigabit network SINET3 supported by National Institute of Informatics for efficient data transfer through Japan Lattice Data Grid (JLDG). This work is supported in part by the Grant-in-Aid of the Ministry of Education (Nos. 18340075, 18740167, 19540286, 19740121, 19740160, 20025010, 20039005, 20740156). The work of HF is supported by Nishina Memorial Foundation.

References

- [1] K. Griest, Phys. Rev. Lett. **61**, 666 (1988). K. Griest, Phys. Rev. D **38**, 2357 (1988) [Erratum-ibid. D **39**, 3802 (1989)].
- [2] A. Bottino, F. Donato, N. Fornengo and S. Scopel, Astropart. Phys. **13**, 215 (2000) [arXiv:hep-ph/9909228].
- [3] J. R. Ellis, K. A. Olive, Y. Santoso and V. C. Spanos, Phys. Lett. B **565**, 176 (2003) [arXiv:hep-ph/0303043]. J. R. Ellis, K. A. Olive, Y. Santoso and V. C. Spanos, Phys. Rev. D **71**, 095007 (2005) [arXiv:hep-ph/0502001].
- [4] E. A. Baltz, M. Battaglia, M. E. Peskin and T. Wizansky, Phys. Rev. D **74**, 103521 (2006) [arXiv:hep-ph/0602187].
- [5] J. Ellis, K. A. Olive and C. Savage, Phys. Rev. D **77**, 065026 (2008) [arXiv:0801.3656 [hep-ph]].
- [6] M. Fukugita et al., Phys. Rev. D **51** (1995) 5319, hep-lat/9408002,
- [7] S.J. Dong, J.F. Lagae and K.F. Liu, Phys. Rev. D **54** (1996) 5496, hep-ph/9602259,
- [8] SESAM, S. Gusken et al., Phys. Rev. D **59** (1999) 054504, hep-lat/9809066,
- [9] C. Michael, C. McNeile and D. Hepburn [UKQCD Collaboration], Nucl. Phys. Proc. Suppl. **106**, 293 (2002) [arXiv:hep-lat/0109028].
- [10] S. Aoki et al. [JLQCD Collaboration], Phys. Rev. D **78**, 014508 (2008) [arXiv:0803.3197 [hep-lat]].
- [11] H. Ohki et al. [JLQCD Collaboration], Phys. Rev. D **78**, 054502 (2008) [arXiv:0806.4744 [hep-lat]].
- [12] A. Walker-Loud et al., arXiv:0806.4549 [hep-lat].
- [13] J. Noaki et al. [JLQCD and TWQCD collaborations], arXiv:0806.0894 [hep-lat].
- [14] E. E. Jenkins and A. V. Manohar, Phys. Lett. B **255**, 558 (1991).
- [15] M. Procura, T. R. Hemmert and W. Weise, Phys. Rev. D **69**, 034505 (2004) [arXiv:hep-lat/0309020]. M. Procura, B. U. Musch, T. Wollenweber, T. R. Hemmert and W. Weise, Phys. Rev. D **73**, 114510 (2006) [arXiv:hep-lat/0603001].
- [16] A. Ali Khan et al. [QCDSF-UKQCD Collaboration], Nucl. Phys. B **689**, 175 (2004) [arXiv:hep-lat/0312030].
- [17] J. W. Chen and M. J. Savage, Phys. Rev. D **65**, 094001 (2002) [arXiv:hep-lat/0111050]. S. R. Beane and M. J. Savage, Nucl. Phys. A **709**, 319 (2002) [arXiv:hep-lat/0203003].
- [18] E. Shintani et al. [for JLQCD Collaboration], arXiv:0806.4222 [hep-lat].
- [19] S. Hashimoto et al. [JLQCD collaboration], PoS **LAT2007**, 101 (2007) [arXiv:0710.2730 [hep-lat]]. H. Matsufuru et al. these proceedings, J. Noaki et al. these proceedings,